HHS Public Access

Author manuscript

*Oncology*. Author manuscript; available in PMC 2017 June 16.

Published in final edited form as:

*Oncology*. 2016 ; 91(2): 90–100. doi:10.1159/000446074.

# Validation of a preclinical model of diethylnitrosamine-induced hepatic neoplasia in Yucatan miniature pigs

**Jennifer Mitchell**[a], **Peggy T. Tinkey**[a], **Rony Avritscher**[b], **Carolyn Van Pelt**[a], **Ghazaleh Eskandari**[c,1], **Suraj Konnath George**[c], **Lianchun Xiao**[e], **Erik Cressman**[b], **Jeffrey S. Morris**[e], **Asif Rashid**[f], **Ahmed O. Kaseb**[g], **Hesham M. Amin**[c,d], and **Rajesh Uthamanthil**[a,2]

[a]Department of Veterinary Medicine and Surgery, The University of Texas MD Anderson Cancer Center, Houston, TX

[b]Department of Interventional Radiology, The University of Texas MD Anderson Cancer Center, Houston, TX

[c]Department of Hematopathology, The University of Texas MD Anderson Cancer Center, Houston, TX

[d]The University of Texas Graduate School of Biomedical Sciences, Houston, TX

[e]Department of Biostatistics, The University of Texas MD Anderson Cancer Center, Houston, TX

[f]Department of Pathology, The University of Texas MD Anderson Cancer Center, Houston, TX

[g]Department of Gastrointestinal Medical Oncology, The University of Texas MD Anderson Cancer Center, Houston, TX

## Abstract

**Objective—**The purpose of this study was to reduce time to tumor onset in a diethylnitrosamine (DEN)-induced hepatocellular carcinoma (HCC) swine model via partial liver embolization (PLE) and to characterize the model for use in translational research.

**Methods—**Eight Yucatan miniature pigs were injected intraperitoneally with either saline (n=2) or DEN (n=6) solution weekly for 12 weeks. Three of the DEN-treated pigs underwent PLE. Animals underwent periodic radiological evaluation, liver biopsy, and blood sampling, and full necropsy was performed at study termination (~29 months).

**Results—**All DEN-treated pigs developed hepatic adenoma and HCC. PLE accelerated the time to adenoma development but not to HCC development. Biomarker analysis results showed that IGF1 levels decreased in all DEN-treated pigs, as functional liver capacity decreased with progression of HCC. VEGF and IL-6 levels were positively correlated with disease progression. Immunohistochemical probing of HCC tissues demonstrated the expression of several important survival-promoting proteins.

**Corresponding author**: Rajesh Uthamanthil, DVM, PhD, DACLAM, Director, Comparative Medicine, Fred Hutchinson Cancer Research Center, P.O. Box 19024, Mailstop CD-101, 1100 Fairview Ave. North, Seattle, WA 98101, Phone: (206) 667-5313, ruthaman@fredhutch.org, Fax: (206) 667-6380.

[1]Current affiliation: Department of Pathology and Immunology, Baylor College of Medicine, Houston, TX.

[2]Current affiliation: Fred Hutchinson Cancer Research Center, Seattle, WA.

**Conclusion—**To our knowledge, we are the first to demonstrate accelerated development of hepatic neoplasia in Yucatan miniature pigs. Our HCC swine model closely mimics the human condition (i.e., progressive disease stages and expression of relevant molecular markers) and is a viable translational model.

### Keywords

hepatocellular carcinoma; Yucatan miniature pigs; diethylnitrosamine; animal models; preclinical studies

## Introduction

The diagnosis of hepatocellular carcinoma (HCC) in humans is challenging because most cases of HCC occur in patients with underlying chronic liver disease, with varying degrees and combinations of fatty changes, fibrosis, and cirrhosis [1]. Distinguishing between nonneoplastic chronic liver disease and HCC is sometimes difficult because histopathologic confirmation of HCC by liver biopsy is the only definitive method of diagnosis. Relevant animal models are needed to develop tests that allow early diagnosis of hepatic neoplasia and more precise discrimination between nonneoplastic chronic liver disease and HCC.

Much progress has been made on the identification of early genetic alterations, important cellular pathways, and molecular changes leading to HCC in rodent models, the most common HCC animal model [2]. However, owing to rodents' small size, researchers are unable to obtain multiple serial samples (i.e., blood or tissue) throughout disease progression from chronic liver disease to HCC. Considerable differences in anatomy, physiology, and mechanisms of carcinogenesis limit the usefulness of rodent models for translational studies in HCC. Well-characterized large animal models that have anatomical and radiological clinical relevance to humans are needed [3].

Owing to the comparable size and function of pig and human livers, swine models play a significant role in hepatology research ranging from physiology to transplantation studies [4]. Additionally, the longer life span of pigs compared with rodents supports long-term research. Recent developments such as the sequencing and manipulation of the pig genome, the development of transgenic pigs, and the development of induced pluripotent swine stem cells have made the swine model an even more powerful translational research tool in hepatology [5–9].

A well-characterized HCC swine model that can be reliably reproduced is needed to support the clinical translation of preventive, diagnostic, and therapeutic discoveries in HCC. Chemical induction of hepatic cancer by diethylnitrosamine (DEN) has been demonstrated in various species, including pigs [10]. However, the usefulness of this model in pigs has been limited by the length of time needed to create the model and the lack of data on its biological characteristics. The purpose of this study was to reduce time to tumor onset in a DEN-induced HCC model in Yucatan miniature pigs via partial liver embolization (PLE) and to characterize this model for use in translational research. We also investigated the expression in this model of survival-promoting proteins (GH, IGF1, JAK2, STAT3, and STAT5) and biomarkers (VEGF, IL-6, and AFP) that are useful for human HCC diagnosis.

## Materials and Methods

### Animals

All procedures performed on animals were approved by the Institutional Animal Care and Use Committee at The University of Texas MD Anderson Cancer Center and were conducted according to the guidelines set forth in the *Guide for the Care and Use of Laboratory Animals* [11]. Eight female specific-pathogen-free Yucatan miniature pigs (*Sus scrofa*; 5–9 weeks old) were purchased from a commercial vendor of laboratory swine (Lonestar Swine/Exemplar Genetics, Sioux Center, IA). Pigs were housed in indoor runs and were exposed to an electronically controlled 12:12 light-dark cycle. The pigs were initially maintained at 78°F±2°F until 16 weeks of age and then were maintained at 72°F±2°F for the remainder of the study. The animals were fed a commercial laboratory diet (Purina LabDiet, St. Louis, MO) and were provided water ad libitum. Upon initiation of the study, the pigs were separated into three groups: Control (n=2), DEN alone (n=3), and DEN+PLE (n=3). A veterinarian clinically observed all pigs daily. Body weight was recorded at least once per month.

### DEN administration

DEN (0.95 g/mL; Sigma-Aldrich, St. Louis, MO) was stored in a light-protected container at 4°C. On the day of administration, the stock solution was diluted in sterile 0.9% sodium chloride solution to yield a final concentration of 50 mg/mL and was injected within 12 h. Remaining diluted solution was discarded.

For each treatment, pigs were anesthetized, weighed, and placed in a dorsal recumbent position. Pigs in the control group received intraperitoneal injections of 0.9% saline solution weekly for 12 weeks. Pigs in the DEN alone group received 12 weekly doses of intraperitoneal DEN (10 mg/kg). Pigs in the DEN+PLE group received 2–4 doses of DEN weekly (10 mg/kg) before PLE and then received a single reduced dose (5 mg/kg) 3–5 days after PLE. Subsequent weekly doses of DEN (10 mg/kg) were given for a total of 12 doses. For both groups, the total cumulative dose of DEN was approximately 2500 mg/pig.

### Anesthesia

For all procedures, pigs were anesthetized via intramuscular injection with either tiletamine-zolazepam (6 mg/kg; Zoetis, Florham Park, NJ) in a mixture of ketamine hydrochloride (15 mg/kg) and acepromazine maleate (0.15 mg/kg). At the time of anesthesia, atropine sulfate (0.04 mg/kg) was also intramuscularly injected. For imaging, surgical procedures, and biopsy, pigs were maintained on isoflurane (1.5%–2.0%) and oxygen (0.8–1.5 L/min). A 22-gauge intravenous catheter was placed in an auricular vein for injection of the contrast material.

### Partial liver embolization

The portal vein blood supply to approximately 70% of the liver was occluded using a transhepatic technique for portal vein embolization, as described previously [12]. Briefly, a scout abdominal radiograph was obtained before catheterization. Using sonographic guidance, a 22-gauge Chiba needle (Neff Percutaneous Access Set; Cook Medical, Inc.,

Bloomington, IN) was inserted percutaneously and advanced through the liver into a branch of the right portal vein. Under fluoroscopic guidance, a 0.018-inch guidewire was advanced into the main portal vein, and the needle was removed. A 5-F flush catheter was then advanced over the wire into the main portal vein. Portography was performed to delineate portal venous anatomy. The flush catheter was then exchanged for a 5-F angled Kumpe access catheter (Cook Medical, Inc., Bloomington, IN). Under fluoroscopic monitoring, embolic particles (355–500 μm; Boston Scientific, Marlborough, MA) suspended in diluted contrast medium (20 mL; 50% contrast and 50% saline solution) were injected into the portal vein branches supplying the left lateral lobe and left medial lobe until near stasis of flow was achieved. Following particulate embolization, metallic vascular occluding coils ranging from 5 mm to 12 mm were deployed within proximal secondary portal vein branches. Portography via the main portal vein was repeated to verify technical success. After completion of the PLE, coils were placed within the tract to prevent hemorrhage.

### Computed tomography

Serial computed tomography (CT) images were obtained every 30–60 days beginning at baseline (i.e., before the first DEN or saline solution administration). Plain and contrast-enhanced whole-body CT imaging was performed on a multi-detector 4-slice helical scanner (LightSpeed Plus; General Electric Medical Systems, Milwaukee, WI) using 3.57-mm slices. For contrast studies, a total of 25 mL of angiographic contrast (Conray 60; Mallinckrodt, Inc., St. Louis, MO) was injected at a rate of 2.5 mL/s through the auricular vein catheter. After a 12-s delay, arterial and venous CT images of the liver were acquired, followed by a total body scan. Images were reconstructed at 2.5-mm slice thickness in the axial plane using a standard soft tissue algorithm. CT images were evaluated for development and progression of cirrhosis and early-stage and late-stage tumors in the liver.

### Liver biopsies

All pigs underwent a series of image-guided liver biopsies beginning 1 month after the first treatment. Biopsies were obtained at 1-month intervals for the first 6 months and then at 2-month intervals until the end of the study. For most pigs, a total of 20–24 biopsies were obtained. Most of the pigs that received DEN had received 5 doses at the time of the first liver biopsy. Biopsy sites were selected on the basis of the CT scan, which was performed just before the biopsy. A 16–18-gauge core biopsy needle was placed percutaneously into the hepatic parenchyma using either CT or ultrasonography guidance. Biopsy samples were fixed in 10% formalin or snap frozen in liquid nitrogen and stored at −80°C. Biopsy samples representing early, middle, and late-stage time points of the experiment were evaluated histologically.

### Blood samples

Blood was collected from the pigs on a monthly basis for complete blood count and serum chemistry, usually in conjunction with imaging or biopsy procedures. Venous blood (5–10 mL) was obtained from a peripheral vein. Samples were analyzed using the Roche Cobas Integra 400+ Chemistry analyzer (Basel, Switzerland) and the ADVIA 120 analyzer (Siemens Healthcare, Malvern, PA). Residual serum was aliquoted and frozen at −80°C for biomarker analysis.

### Enzyme-linked immunosorbent assay

Commercially available enzyme-linked immunosorbent assay kits were purchased from Biomatik Corporation (Cambridge, ON, Canada). The kits were used to measure the levels of GH (EKU04610), IGF1 (EKU04969), IGF2 (EKU04978), AFP (EKU02293), VEGFA (EKU08092), and IL-6 (EKU05362) in fresh frozen serum samples collected from the pigs. The samples were diluted in phosphate-buffered saline solution to 0.01 mol/L (pH, 7.2) if required (1:3 for GH, 1:200 for IGF1, and 1:50 for IGF2). Optical density was measured using a microplate enzyme-linked immunosorbent assay reader with a 450-nm filter.

### Necropsy

Approximately 29 months after initiation of the study, two of the pigs in the DEN+PLE group died owing to complications unrelated to the study. The study was terminated at that time, and the remaining animals were euthanized by an intravenous overdose of a commercial euthanasia solution (Beuthanasia-D special, Merck Animal Health, Summit, NJ). All animals underwent necropsy, major organ systems were visually examined, and lesions were noted. Samples from each liver lobe were collected and fixed in 10% formalin.

### Histopathology

Liver biopsies and post-mortem liver tissues were stained with hematoxylin and eosin. Specimens with pathologic lesions were stained with reticulin and trichrome for further analysis. All tissues were evaluated by board-certified pathologists (CVP, AR, and HMA).

### Immunohistochemistry

Biopsied liver samples obtained between 1 month and 6 months after the first treatment were immunostained with Ki67 antibody to evaluate the proliferative index of hepatocytes. Total hepatocyte nuclei and Ki67-positive hepatocyte nuclei in six random high-power fields from each biopsied sample were counted automatically using a macro program (Image-Pro, Meyer Instruments, Inc., Houston, TX). Once the program tabulated the total and Ki67-positive hepatocyte nuclei, the operator viewed each field to determine whether the counted cells were hepatocyte nuclei and corrected the counts if needed. The proliferative index for hepatocytes was calculated as the number of Ki67-positive nuclei per 1000 nuclei.

The following antibodies were purchased: GHR (ab11380), STAT5 (A+B; ab194898), pSTAT5 (Tyr694; ab32364), and pIGF1R (Tyr1161; ab39398; Abcam, Cambridge, MA); IGF1Rβ (sc-713), STAT3 (sc-8019), and pJAK2 (Tyr1007/Tyr1008; sc-21870; Santa Cruz Biotechnology, Dallas, TX); and JAK2 (3230) and pSTAT3 (Tyr705; 4113; Cell Signaling Technology, Danvers, MA). Immunohistochemical staining was performed on formalin-fixed and paraffin-embedded tissue sections from the swine livers using a standard approach as previously described [13]. Initial deparaffinization was performed using an alcohol gradient. After washing the samples in phosphate-buffered saline solution (0.5% Tween), antigen retrieval was performed for 20 min in a steamer using Target Retrieval Solution (Dako, Carpinteria, CA), and then the samples were allowed to cool to room temperature for 20 min. Endogenous peroxidase activity was blocked with 3% hydrogen peroxide, and the sections were then blocked in serum-free blocking solution (Universal LSAB+ kit, Dako) for 30 min for GHR and STAT3 antibodies and for 2 h for IGF1Rβ antibody. The primary

antibodies were diluted in blocking buffer (GHR, 1:100; IGF1Rβ, 1:150; JAK2, 1:400; STAT3, 1:50; STAT5, 1:2000; pJAK2, 1:100; pSTAT3, 1:25; and pSTAT5, 1:75) and were applied to the slides, which were then incubated overnight at 4°C. Slides were then treated for 30 min with secondary antibody LINK (Dako) and then were developed with 3,3′-diaminobenzidine tetrahydrochloride substrate with horseradish peroxidase. Counterstaining was performed using hematoxylin. Photomicrographs were captured using a Nikon Microphot FXA microscope (Nikon Instruments, Melville, NY), an Olympus DP70 camera (Olympus America, Center Valley, PA), and QCapture Suite PLUS software (QImaging, Surrey, BC, Canada).

### Statistical analysis

All statistical analyses were performed using SAS software (SAS Institute, Inc., Cary, NC) and S-Plus software (TIBCO Software, Inc., Palo Alto, CA). The Kaplan-Meier method and log-rank test were used to evaluate the time to neoplasia occurrence among the two treatment groups (DEN alone or DEN+PLE). Spearman correlation coefficients were calculated to estimate associations among the serum biochemical markers. Linear mixed models with group, time, and the interaction of group and time as fixed effects were fitted to evaluate changes of marker expression over time in each treatment group. To account for correlation among markers from the same pig measured over time, the experimental pigs were included as a random effect in the linear mixed models. Log-transformed marker values were used for model fitting. P values less than 0.05 were considered statistically significant.

## Results

### Physical appearance and body condition

All pigs exhibited normal appearance, appetite, and body condition throughout the study. The average final body weight was 58 kg in the control group, 64 kg in the DEN alone group, and 62 kg in the DEN+PLE group, all of which were consistent with normal, mature body weight in this species [14]. None of the pigs exhibited clinical signs of hepatic dysfunction during the study.

### Imaging

Serial multiphase CT scans of the abdomen were obtained from each animal. In control animals, no abnormalities were identified in the liver during the study. Homogeneous parenchymal enhancement was observed in arterial and portal venous phases, and all major vessels were readily apparent. The liver extended laterally to the left abdominal wall in every animal, and in most cases the spleen extended to the right abdominal wall.

In the DEN-treated groups, perfusion abnormalities were observed with gradual growth of lesions over several months. The parenchymal enhancement patterns changed considerably during the study; within 12–14 months, we observed heterogeneous and irregular patterns, which became more pronounced over time.

In the DEN+PLE group, mixed results were observed regarding degree of atrophy of the embolized portion of the liver and hypertrophy of the remnant liver. The changes occurred within several weeks after embolization and remained stable thereafter. In one animal, the atrophy/hypertrophy changes resulted in a persistent medial shift of the gallbladder, as demonstrated in figure 1. The portal vein in the animals that received PLE did not enhance well and, in some cases, was not easily identified even in the nonembolized region. With respect to lesion distribution, numerous enhancing lesions were identified in all liver lobes in all DEN-treated animals regardless of whether the portal vein was embolized. It was not possible to distinguish between nodules with different degrees of dysplasia. Adenomas and carcinomas had a similar appearance on the imaging findings.

### Complete blood counts and serum chemistry

There were no significant differences in complete blood count and serum chemistry between the control and DEN-treated groups or between the two DEN-treated groups (data not shown).

### Gross pathology

At necropsy, the pigs were in a good nutritional state with moderate amounts of subcutaneous and intra-abdominal fat deposits. The livers of the control pigs were of normal size, weight, and appearance on both the capsular and cut surfaces. The livers of DEN-treated pigs had similar gross appearance with a pale, irregular gray color and an indurated and pitted capsular surface (fig. 2). DEN-treated pigs had smaller livers than the control pigs. In the DEN+PLE pigs, the left lobes were markedly larger than the embolized right lobes. On the cut surfaces, livers of the DEN-treated pigs contained multiple nodules of varying size and shape that were separated by thick cords of fibrous tissue. The gallbladders appeared normal.

### Histopathology

Histopathologic changes in the liver tissue were observed starting 5 weeks after initiating DEN injections. These changes consisted of mild, mixed inflammatory cell infiltrates (i.e., neutrophils and mononuclear cells) and increased eosinophilic granularity of hepatocellular cytoplasm typically observed after xenobiotic administration that results in enzyme induction. Foci of altered hepatocytes (clear, eosinophilic, or mixed) were observed in both DEN-treated groups as early as 9 months after study initiation and were observed in all post-mortem liver tissue from the DEN-treated pigs. These foci were presumptive preneoplastic lesions that varied from barely perceptible to cytomorphologically and tinctorially discrete lesions. Foci typically blended imperceptibly with and did not compress surrounding hepatic parenchyma, though minimal compression occasionally occurred. Foci were classified on the basis of hematoxylin and eosin tinctorial properties and cytoplasmic features [15]. One pig from the control group had foci of cellular alteration (clear or mixed) in post-mortem tissue, but not in the biopsied samples. Neoplastic lesions were observed in all DEN-treated pigs at several time points throughout the study, but no neoplastic lesions were observed in either of the control animals during the study.

Hepatocellular adenomas (singular and multiple) occurred in all six DEN-treated pigs. The adenomas were composed of well-demarcated nodules of normal-appearing hepatocytes that varied in size and tinctorial characteristics. These nodules lacked normal lobular architecture: central veins and portal tracts were not readily apparent. In some adenomas, cellular atypia, basophilia, and vacuolization of the cytoplasm were observed. A carcinoma arising within an adenoma was observed in one of the pigs treated with DEN alone.

Hepatocellular carcinomas (singular and multiple) were observed in all six DEN-treated pigs. Carcinomas consisted of neoplastic hepatocytes that approximated the appearance of normal hepatocytes but varied in size and tinctorial appearance (fig. 3). The growth pattern was mostly trabecular, with thickened hepatic cords (2–3 cells thick). Frequently, the pattern was trabecular/glandular and trabecular/compact.

Sarcomas were observed in two of the DEN+PLE pigs. These were diffuse infiltrations of histiocytic appearing cells (data not shown). Immunophenotyping of the sarcoma lesions was not performed; therefore, the lesions were classified as sarcoma, not otherwise specified.

The DEN+PLE pigs showed a robust regenerative response that was confirmed by an increase in Ki67-positive hepatocytes (data not shown). The hepatocellular proliferation index indicated an increase in cellular proliferation starting at approximately 1 month from initiation of DEN administration in the treated groups. The proliferation index was greatest in the DEN+PLE group, followed by the DEN group and was least in the control group. At 10 months, the proliferation index level was lower than the initial values observed in the first 3 months after DEN administration, but both DEN-treated groups maintained a slightly higher proliferation index over the 10–11 months it was measured than that of the control group at 9 months.

### Tumor latency

Neither of the two control pigs developed hepatic neoplasia. All DEN-treated pigs showed progressive hepatitis, bile duct hyperplasia, hepatic lipidosis (steatosis), fibrosis (predominantly in the peribiliary region), and cirrhosis that progressed throughout the course of the study. Starting at approximately 9 months after the first DEN injection, two of the three pigs in the DEN+PLE group developed putative preneoplastic lesions (i.e., foci of hepatocellular alteration [clear or eosinophilic]). By month 15, all DEN-treated pigs developed foci of altered hepatocytes (clear, eosinophilic, or mixed; data not shown). The first incidence of hepatocellular neoplasia (i.e., hepatocellular adenoma) was confirmed at 15 months in the DEN+PLE group via CT-guided biopsy. HCC was first confirmed in the same animal at 18 months. At the end of the study (29 months), hepatocellular adenomas and HCC were both observed in all six DEN-treated pigs.

The mean time to hepatic neoplasia was 15.97 months in the DEN+PLE group compared with 27.65 months in the group treated with DEN alone (fig. 4). Kaplan-Meier estimate and log-rank test results indicated that pigs treated with DEN+PLE developed hepatic neoplasia more quickly than pigs treated with DEN alone ($p=0.0246$; fig. 4).

### Biomarkers

Serum samples from four time points (baseline, 6 months, 15 months, and 25 months) were chosen for analysis. Values for each biomarker (AFP, GH, IGF1, IGF2, VEGF, and IL-6) were evaluated to determine expression under different treatment conditions over time and to determine whether there was any association among biomarkers.

IGF1 levels in the control group remained stable and did not change significantly during the study. Compared with baseline levels, the IGF1 levels in both DEN-treated groups gradually decreased during the study. IGF1 levels in both DEN-treated groups were significantly lower than in the control group ($p<0.05$; fig. 4). VEGF levels increased from baseline in both DEN-treated groups compared with the control group (DEN alone, $p<0.0279$; DEN+PLE, $p<0.0057$; VEGF levels not shown).No significant changes in the other biomarkers were observed among the three swine groups.

GH and AFP were positively correlated, with an estimated correlation coefficient of 0.425 ($p=0.017$), and VEGF and IL-6 were positively correlated, with an estimated correlation coefficient of 0.516 ($p=0.003$). Table 1 shows the estimated Spearman correlation coefficients between biomarkers of all pigs. No other significant correlations were detected.

### Immunohistochemistry

Immunohistochemical staining results showed the expression of important cell survival proteins that have been previously demonstrated in HCC, including GHR and tyrosine kinases and transcription factors JAK2, STAT3, STAT5, and IGF1R [16–23]. Additionally, the activated/phosphorylated forms of these kinases and transcription factors were also detected (fig. 3). Generally, the expression of these proteins was more pronounced in the HCC tissue than in the non-cancerous tissue (data not shown).

## Discussion

To our knowledge, we are the first to demonstrate accelerated development of hepatic neoplasia in Yucatan miniature pig models and to report potential biomarkers of human relevance in a HCC swine model. Previously reported swine studies have been limited by the time to development of hepatic neoplasia [24]; therefore, we attempted to accelerate the development of hepatic neoplasia by administering DEN during rapid hepatic regeneration induced by PLE. Since a previously reported DEN-induced HCC swine model study generated limited radiographic and histopathologic data [25], we characterized the model through serial analysis of radiographic changes, serum biomarkers, and tissue expression of major survival-promoting proteins associated with human HCC.

Our swine model demonstrated a step-wise progression in lesions from inflammation, fibrosis/cirrhosis, preneoplastic lesions, hepatic adenoma, and HCC. The course of disease in this model reflects several aspects of HCC development in humans, thus confirming its utility for translational research to refine imaging techniques and investigate possible biomarkers that could improve the diagnosis and prognosis of HCC.

Both DEN-treated groups developed hepatocellular neoplasia similar to those observed in humans [26]. Foci of altered hepatocytes (clear, eosinophilic, or mixed), which are considered presumptive preneoplastic lesions in human and rodent livers [26], were observed in both DEN-treated groups, with the earliest focus observed at 9 months. Therefore, it can be assumed that the foci of alteration in the DEN-treated pigs were presumptive preneoplastic lesions. Two foci were also observed in a control pig. However, foci of alteration have been reported to occur spontaneously in miniature pigs secondary to glycogen accumulation [27] and in control rodents in long-term studies and have not been associated with administration of chemicals [15]. Since most liver sections from this control pig had no significant lesions, these foci were considered spontaneous.

The main difference between the two DEN-treated groups was the time to onset of hepatic adenomas. PLE accelerated the onset of adenomas in DEN-treated animals. The PLE technique caused hepatic responses similar to those that occur in the rodent partial hepatectomy model for carcinogenesis assays [28]. Although biopsied samples taken in the first year of our study demonstrated an increase in hepatocellular proliferation in the two DEN-treated groups, the DEN+PLE group was the first group to develop preneoplastic and neoplastic hepatocellular lesions and had the highest increase in cell proliferation.

Notably, the time to HCC development in our study was similar to or longer than previously reported data [25]. While Li et al. noted the occurrence of cirrhosis in their model, they concluded that most radiographic lesions were HCC. In our study, many of the radiographic lesions were primarily areas of fibrosis and nodular hepatic regeneration, with small, scattered areas of HCC present within this widespread framework of hepatic response. It is likely that HCC was present in the pigs at earlier time points than was confirmed by biopsy even though biopsied areas were selected on the basis of radiographic evidence of disease. This result closely mimics the human condition, in which HCC is difficult to diagnose by ultrasonography, CT, or magnetic resonance imaging. Multiple biopsies often are required to confirm the presence of HCC in patients [29]; it is precisely this difficulty in diagnosing HCC that drives current research efforts to find new biomarkers and imaging techniques that can be used for early diagnosis.

Previous studies have demonstrated the expression of several important survival-promoting proteins in HCC. For instance, recent findings from our group suggest that the GHR/IGF1 signaling axis plays an important role in HCC [30]. In our current study, the expression of GHR and IGF1R was very pronounced in the HCC tissue from DEN-treated pigs. Moreover, the expression of GHR/IGF1R downstream signaling molecules, including JAK2, STAT3, and STAT5, was also detected in HCC tissue from DEN-treated pigs, which supports previous studies that have proposed that these molecules play important roles in the survival of human HCC [16–23]. Importantly, the phosphorylated/activated forms JAK2, STAT3, STAT5, and IGF1R were also expressed in HCC tissues from the DEN-treated pigs.

A novel aspect of our study was the assessment of serum-based biomarkers throughout the progression of disease. It was previously reported that this model exhibited elevated serum AFP levels [25], and we obtained similar results. However, AFP levels have poor specificity as a marker for HCC [31]. The need to discover specific biomarkers for diagnosis,

prognosis, and therapy response in HCC patients has been highlighted in several recent studies, which have demonstrated improved prediction of overall survival and patient stratification by including plasma or serum biomarkers, such as VEGF, IGF1, and GH, in established scoring systems [32–36]. The Child-Turcotte-Pugh score is the standard prognostic method used to evaluate hepatic reserve and guide therapy decisions for patients with HCC and advanced chronic liver disease. It has been suggested that modifying the Child-Turcotte-Pugh score by replacing the current assessment of encephalopathy and severity of ascites with plasma IGF1 levels would improve the accuracy of survival prediction and stratification of patients in clinical trials; however, a strategy for use of IGF1 levels in clinical practice is still lacking [37].

In humans, IGF1 is produced primarily by the liver and is an indirect measure of hepatic reserve [37]. While the levels of IGF1 remained stable in the control pigs, these levels decreased significantly in both DEN-treated groups. Most likely, these findings can be attributed to the fact that treatment with DEN, with or without PLE, produces substantial liver necrosis with progressive fibrosis and cirrhosis; thus, decreased IGF1 levels correlated with decreased functional capacity of the liver in the DEN-treated pigs. We expected that, as IGF1 levels decreased, GH levels would increase because of the negative feedback effects of the decreased IGF1 levels on the pituitary gland, similar to recent observations reported by our group [30]. Our current study, however, did not demonstrate a negative correlation between GH and IGF1. This finding may have resulted from various factors, including the small sample size, potential for diurnal variation on the basis of time of sample collection, and age of the pigs at the start of the study. We used pigs aged 5–9 weeks because liver cancer induction is more effective when hepatocytes are rapidly dividing (as occurs in young, growing animals) and because young laboratory pigs are more commonly available from vendors than mature animals. However, GH levels in young, rapidly growing animals are higher than in mature animals [38]; thus, failure to demonstrate a negative correlation between GH and IGF1 may have resulted from the age of the pigs and the time of sample collection.

HCC is a highly vascular tumor that frequently expresses VEGF. Because VEGF levels progressively increase throughout HCC development from low-grade to high-grade dysplasia to HCC, researchers have suggested that VEGF could be used as a biomarker in HCC for screening and monitoring treatment response in patients [39]. Over the course of our study, the VEGF serum levels in the DEN-treated pigs were higher than in the control group. Although the IL-6 levels did not significantly differ between the control and treatment groups, VEGF and IL-6 levels were positively correlated. IL-6 is an important contributor to the development of HCC in rodent models and is used as a biomarker to predict the development of HCC in patients with chronic hepatitis B infection [40, 41]. Our data suggest that IL-6 may also play a role in HCC development in the swine model, suggesting that this model is a valid translational tool that resembles HCC in humans.

Because our carcinogen-induced HCC swine model mimics many aspects of human HCC at both the organ and cellular level, this model could be useful for translational research. Future studies are needed to refine the model and increase its utility, such as shortening the time to tumor latency. For example, using higher doses and/or shorter dosing intervals of

DEN than those used in our study, either alone or in combination with PLE, could reduce tumor latency. To assess the GH/IGF1 axis, future studies should consider using mature pigs with stable levels of GH and a standard sample collection time. Future studies are needed to refine the swine model to induce both HCC and nonalcoholic fatty liver disease/nonalcoholic steatohepatitis for translational studies to address the increasing number of patients in the US who develop HCC without viral hepatitis and/or cirrhosis. Recent studies have shown that existing HCC grading systems, such as the Barcelona Clinic Liver Cancer and the Cancer of the Liver Italian Program systems, are less useful for these patients. Swine are an established model of diet-induced fatty liver disease and metabolic syndrome [42], and a swine model of metabolic syndrome with concurrent HCC would be a valuable tool in translational studies for future biomarker development. Finally, the recent development of genetically engineered pigs may allow mutation of selected genes to rapidly induce HCC in a large animal model with demonstrated relevant physiology to humans, which will enable serial collection of blood and tissue samples [43, 44].

## Acknowledgments

This research was supported in part by the GS Hogan Foundation and The University of Texas MD Anderson Cancer Center. Additional support was provided by the National Institutes of Health through the MD Anderson Cancer Center Support Grant (CA016672). HMA is supported by a National Cancer Institute grant (R01CA151533). The contents of this paper are solely the responsibility of the authors and do not necessarily represent the official views of the National Cancer Institute or the National Institutes of Health.

We thank Prashasnika Gehlot, Dana Toomey, Darla Stange, and Katherine Dixon for their technical assistance and Jill Delsigne for her assistance in editing the manuscript.

## References

1. Llovet JM, Burroughs A, Bruix J. Hepatocellular carcinoma. Lancet. 2003; 362:1907–1917. [PubMed: 14667750]
2. Newell P, Villanueva A, Friedman SL, Koike K, Llovet JM. Experimental models of hepatocellular carcinoma. J Hepatol. 2008; 48:858–879. [PubMed: 18314222]
3. Li X-J, Li W. Beyond mice: Genetically modifying larger animals to model human diseases. Journal of Genetics and Genomics. 2012; 39:237–238. [PubMed: 22749009]
4. Swindle, MM. Liver and biliary system. In: Swindle, MM., Smith, AC., editors. Swine in the laboratory: Surgery, anesthesia, imaging, and experimental techniques. 3rd. Boca Raton, FL: CRC Press; 2015. p. 135-154.
5. Aigner B, Renner S, Kessler B, Klymiuk N, Kurome M, Wünsch A, et al. Transgenic pigs as models for translational biomedical research. J Mol Med. 2010; 88:653–664. [PubMed: 20339830]
6. Groenen MAM, Archibald AL, Uenishi H, Tuggle CK, Takeuchi Y, Rothschild MF, et al. Analyses of pig genomes provide insight into porcine demography and evolution. Nature. 2012; 491:393–398. [PubMed: 23151582]
7. Esteban MA, Xu J, Yang J, Peng M, Qin D, Li W, et al. Generation of induced pluripotent stem cell lines from tibetan miniature pig. J Biol Chem. 2009; 284:17634–17640. [PubMed: 19376775]
8. Ezashi T, Telugu BPV, Alexenko AP, Sachdev S, Sinha S, Roberts RM. Derivation of induced pluripotent stem cells from pig somatic cells. Proc Natl Acad Sci U S A. 2009; 106:10993–10998. [PubMed: 19541600]
9. Montserrat N, Bahima E, Batlle L, Häfner S, Rodrigues A, González F, et al. Generation of pig ips cells: A model for cell therapy. J Cardiovasc Transl Res. 2011; 4:121–130. [PubMed: 21088946]
10. Verna L, Whysner J, Williams GM. N-nitrosodiethylamine mechanistic data and risk assessment: Bioactivation, DNA-adduct formation, mutagenicity, and tumor initiation. Pharmacol Ther. 1996; 71:57–81. [PubMed: 8910949]

11. National Research Council. Guide for the care and use of laboratory animals. 8th. Washington, DC: National Academies Press; 2011.
12. Madoff DC, Gupta S, Pillsbury EP, Kan Z, Tinkey PT, Stephens LC, et al. Transarterial versus transhepatic portal vein embolization to induce selective hepatic hypertrophy: A comparative study in swine. J Vasc Interv Radiol. 2007; 18:79–93. [PubMed: 17296708]
13. George SK, Vishwamitra D, Manshouri R, Shi P, Amin HM. The alk inhibitor asp3026 eradicates npm-alk+ t-cell anaplastic large-cell lymphoma in vitro and in a systemic xenograft lymphoma model. Oncotarget. 2014; 5:5750. [PubMed: 25026277]
14. Swindle, MM. Liver and biliary system. In: Swindle, MM., Smith, AC., editors. Swine in the laboratory: Surgery, anesthesia, imaging, and experimental techniques. 3rd. Boca Raton, FL: CRC Press; 2015. p. 5
15. Thoolen B, Maronpot RR, Harada T, Nyska A, Rousseaux C, Nolte T, et al. Proliferative and nonproliferative lesions of the rat and mouse hepatobiliary system. Toxicol Pathol. 2010; 38:5S–81S. [PubMed: 21191096]
16. Lincoln D, Sinowatz F, Temmim-Baker L, Baker HI, Kölle S, Waters MJ. Growth hormone receptor expression in the nucleus and cytoplasm of normal and neoplastic cells. Histochem Cell Biol. 1998; 109:141–159. [PubMed: 9504775]
17. García-Caballero T, Mertani HM, Lambert A, Gallego R, Fraga M, Pintos E, et al. Increased expression of growth hormone and prolactin receptors in hepatocellular carcinomas. Endocrine. 2000; 12:265–271. [PubMed: 10963047]
18. Fu X-T, Dai Z, Song K, Zhang Z-J, Zhou Z-J, Zhou S-L, et al. Macrophage-secreted il-8 induces epithelial-mesenchymal transition in hepatocellular carcinoma cells by activating the jak2/stat3/snail pathway. Int J Oncol. 2015; 46:587–596. [PubMed: 25405790]
19. Siveen K, Nguyen A, Lee J, Li F, Singh S, Kumar AP, et al. Negative regulation of signal transducer and activator of transcription-3 signalling cascade by lupeol inhibits growth and induces apoptosis in hepatocellular carcinoma cells. Br J Cancer. 2014; 111:1327–1337. [PubMed: 25101566]
20. Niwa Y, Kanda H, Shikauchi Y, Saiura A, Matsubara K, Kitagawa T, et al. Methylation silencing of socs-3 promotes cell growth and migration by enhancing jak/stat and fak signalings in human hepatocellular carcinoma. Oncogene. 2005; 24:6406–6417. [PubMed: 16007195]
21. Lee TK, Man K, Poon RT, Lo CM, Yuen AP, Ng IO, et al. Signal transducers and activators of transcription 5b activation enhances hepatocellular carcinoma aggressiveness through induction of epithelial-mesenchymal transition. Cancer Res. 2006; 66:9948–9956. [PubMed: 17047057]
22. Chun YS, Huang M, Rink L, Von Mehren M. Expression levels of insulin-like growth factors and receptors in hepatocellular carcinoma: A retrospective study. World J Surg Oncol. 2014; 12:231. [PubMed: 25052889]
23. Yan X-D, Yao M, Wang L, Zhang H-J, Yan M-J, Gu X, et al. Overexpression of insulinlike growth factor-i receptor as a pertinent biomarker for hepatocytes malignant transformation. World journal of gastroenterology: WJG. 2013; 19:6084. [PubMed: 24106410]
24. Graw J, Berg H. Hepatocarcinogenetic effect of dena in pigs. Zeitschrift für Krebsforschung und Klinische Onkologie. 1977; 89:137–143.
25. Li X, Zhou X, Guan Y, Wang Y-XJ, Scutt D, Gong Q-Y. N-nitrosodiethylamine-induced pig liver hepatocellular carcinoma model: Radiological and histopathological studies. Cardiovasc Intervent Radiol. 2006; 29:420–428. [PubMed: 16502159]
26. Thoolen B, Ten Kate FJ, van Diest PJ, Malarkey DE, Elmore SA, Maronpot RR. Comparative histomorphological review of rat and human hepatocellular proliferative lesions. J Toxicol Pathol. 2012; 25:189–199. [PubMed: 22988337]
27. Gad, SC., Dincer, Z., Svendsen, O., Skaanild, MT. The minipig. In: Gad, SC., editor. Animal models in toxicology. 2nd. CRC Press; 2006. p. 731-771.
28. Duncan JR, Hicks ME, Cai S-R, Brunt EM, Ponder KP. Embolization of portal vein branches induces hepatocyte replication in swine: A potential step in hepatic gene therapy. Radiology. 1999; 210:467–477. [PubMed: 10207431]

29. Kojiro M, Wanless IR, Alves V, Badve S, Balabaud C, Bedossa P. Pathologic diagnosis of early hepatocellular carcinoma: A report of the international consensus group for hepatocellular neoplasia. Hepatology. 2009; 49:658–664. [PubMed: 19177576]
30. Abdel-Wahab R, Shehata S, Hassan MM, Habra MA, Eskandari G, Tinkey PT, et al. Type 1 insulin-like growth factor as a liver reserve assessment tool in hepatocellular carcinoma. Journal of Hepatocellular Carcinoma. 2015; 2:131–142. [PubMed: 27508202]
31. Masuzaki, R., Karp, SJ., Omata, M. Semin Oncol. Vol. 39. Elsevier; 2012. New serum markers of hepatocellular carcinoma; p. 434-439.
32. Kaseb AO, Morris JS, Hassan MM, Siddiqui AM, Lin E, Xiao L, et al. Clinical and prognostic implications of plasma insulin-like growth factor-1 and vascular endothelial growth factor in patients with hepatocellular carcinoma. J Clin Oncol. 2011; 29:3892–3899. [PubMed: 21911725]
33. Kaseb JM AO, Hassan M, Lin E, Xiao L, Abdalla EK, Vauthey J, Abbruzzese JL. Iv-hcc: Clinical and prognostic implications of plasma igf-1 and vegf in patients with hepatocellular carcinoma. J Clin Oncol. 2011; 29(suppl 4) abstr 155.
34. Kaseb AO, Abbruzzese JL, Vauthey JN, Aloia TA, Abdalla EK, Hassan MM, et al. I-clip: Improved stratification of advanced hepatocellular carcinoma patients by integrating plasma igf-1 into clip score. Oncology. 2011; 80:373–381. [PubMed: 21822028]
35. Kaseb AO, Hassan MM, Lin E, Xiao L, Kumar V, Pathak P, et al. V-clip: Integrating plasma vascular endothelial growth factor into a new scoring system to stratify patients with advanced hepatocellular carcinoma for clinical trials. Cancer. 2010
36. Rehem RN, El-Shikh WM. Serum igf-1, igf-2 and igfbp-3 as parameters in the assessment of liver dysfunction in patients with hepatic cirrhosis and in the diagnosis of hepatocellular carcinoma. Hepatogastroenterology. 2011; 58:949–954. [PubMed: 21830422]
37. Kaseb AO, Xiao L, Hassan MM, Chae YK, Lee JS, Vauthey JN, et al. Development and validation of insulin-like growth factor-1 score to assess hepatic reserve in hepatocellular carcinoma. J Natl Cancer Inst. 2014
38. Siers DG, Swiger L. Influence of live weight, age and sex on circulating growth hormone levels in swine. J Anim Sci. 1971; 32:1229–1232. [PubMed: 5087371]
39. Kaseb AO HA, Cotant M, Hassan MM, Wollner I, Philip PA. Vascular endothelial growth factor (vegf) in the management of hepatocellular carcinoma (hcc). A review of literature. Cancer. 2009 (In Press).
40. Naugler WE, Sakurai T, Kim S, Maeda S, Kim K, Elsharkawy AM, et al. Gender disparity in liver cancer due to sex differences in myd88-dependent il-6 production. Science. 2007; 317:121–124. [PubMed: 17615358]
41. Wong VWS, Yu J, Cheng ASL, Wong GLH, Chan HY, Chu ESH, et al. High serum interleukin-6 level predicts future hepatocellular carcinoma development in patients with chronic hepatitis b. Int J Cancer. 2009; 124:2766–2770. [PubMed: 19267406]
42. Lee L, Alloosh M, Saxena R, Van Alstine W, Watkins BA, Klaunig JE, et al. Nutritional model of steatohepatitis and metabolic syndrome in the ossabaw miniature swine. Hepatology. 2009; 50:56–67. [PubMed: 19434740]
43. Leuchs S, Saalfrank A, Merkl C, Flisikowska T, Edlinger M, Durkovic M, et al. Inactivation and inducible oncogenic mutation of p53 in gene targeted pigs. PLoS One. 2012; 7:e43323. [PubMed: 23071491]
44. Sieren JC, Meyerholz DK, Wang X-J, Davis BT, Newell JD Jr, Hammond E, et al. Development and translational imaging of a tp53 porcine tumorigenesis model. J Clin Invest. 2014; 124:4052–4066. [PubMed: 25105366]

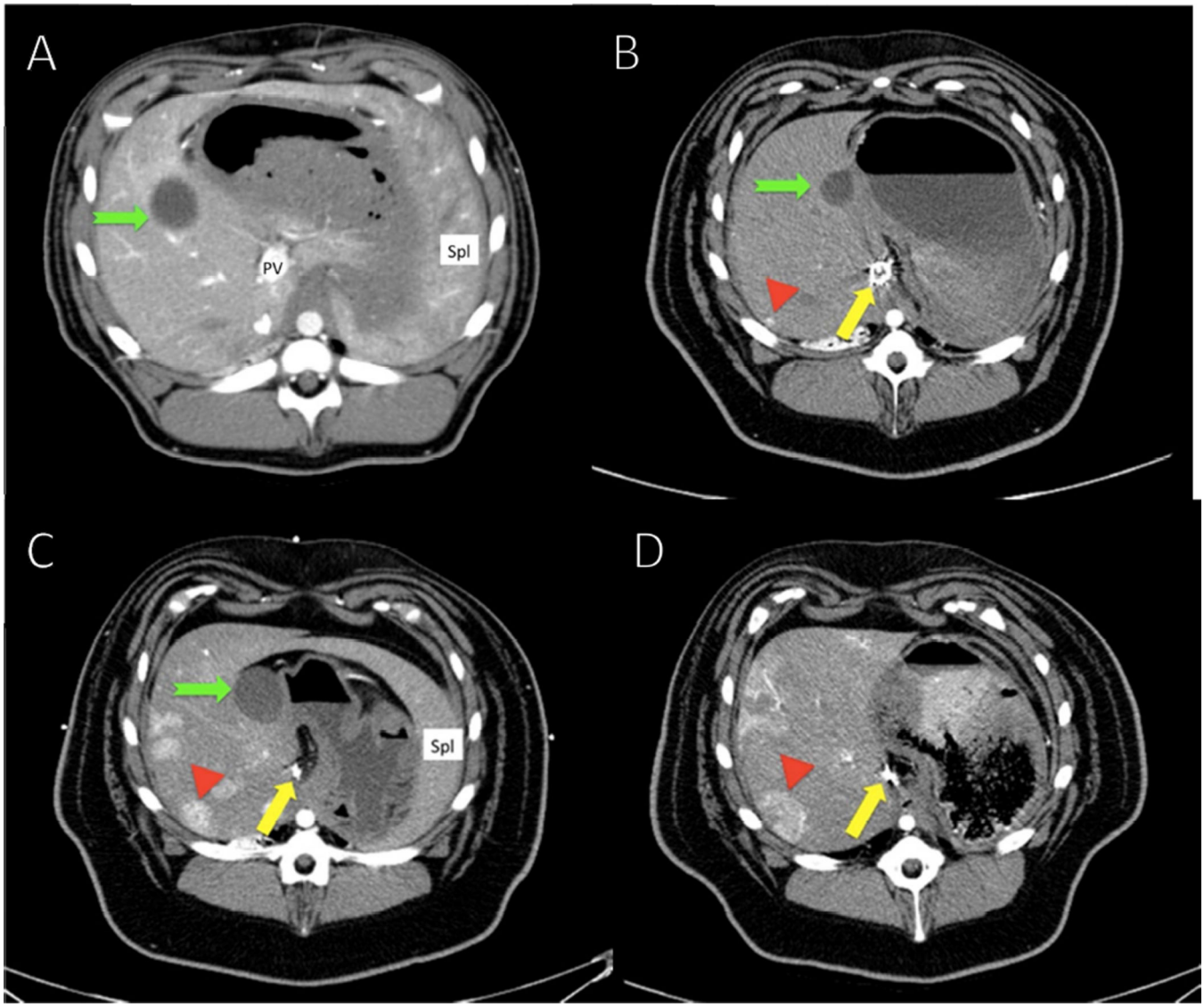


**Fig. 1. Computed tomography studies of hepatocellular carcinoma (HCC) tumors in a representative diethylnitrosamine (DEN)-treated Yucatan miniature pig**

Following embolization and treatment with DEN, the pigs developed focal hypervascular lesions in multiple areas throughout the liver as shown by contrast enhancement (red arrowhead). In keeping with the progression of neoplastic lesions, these lesions culminated in the appearance of nodules, which were histologically shown to be HCC.(A) Baseline scan. During all phases of the initial scan, liver parenchyma enhanced evenly. The portal vein was readily identified on the first scan before embolization but was not well visualized on subsequent studies, particularly in the embolized region. (B) Scan at 16 months shows slight medial shift of the gallbladder owing to the shrinkage of the embolized left side of the liver (green notched arrow). The coils in the portal vein (yellow arrow) and the tumor (red arrowhead) are indicated. (C) Scan at 22 months. Note growth in both size and degree of enhancement of the index lesion and the background of additional similar lesions progressing over time until (D) final scan at 28 months just before the pig was euthanized.

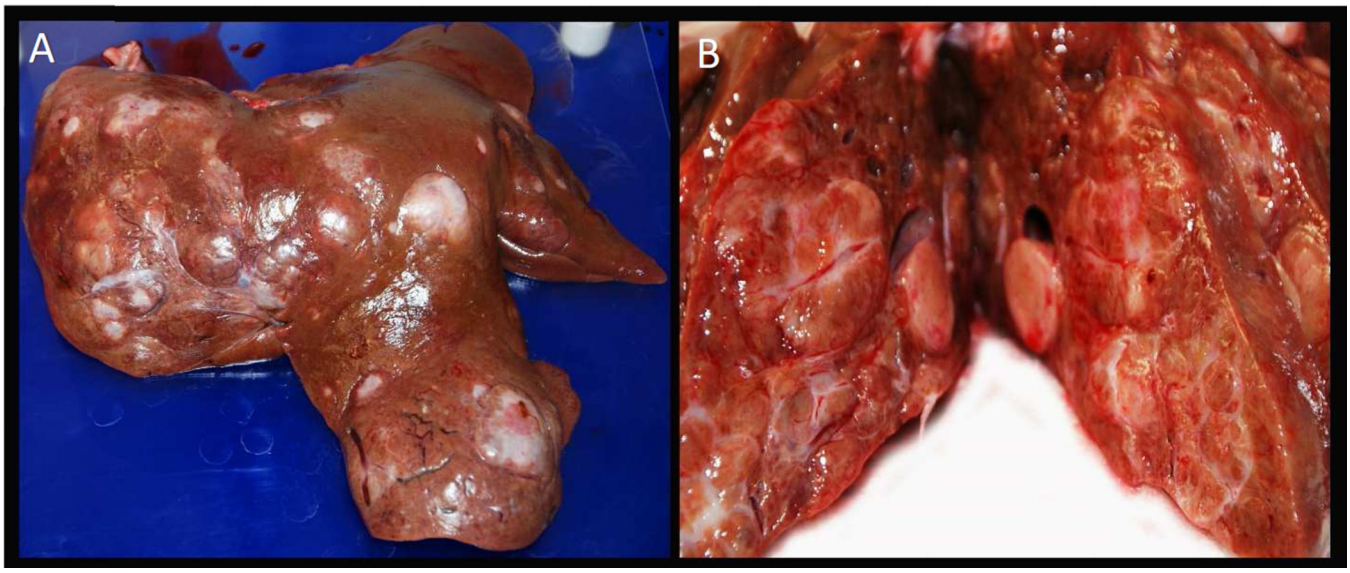


**Fig. 2. Gross pathology of liver from a Yucatan miniature pig treated with diethylnitrosamine (DEN) + partial liver embolization (PLE)**

Gross appearance of the capsular (A) and cut (B) surfaces, respectively, of the liver of a DEN+PLE pig showing extensive diffuse hepatic nodules of varying sizes and distorted capsular surface caused by fibrosis/cirrhosis.

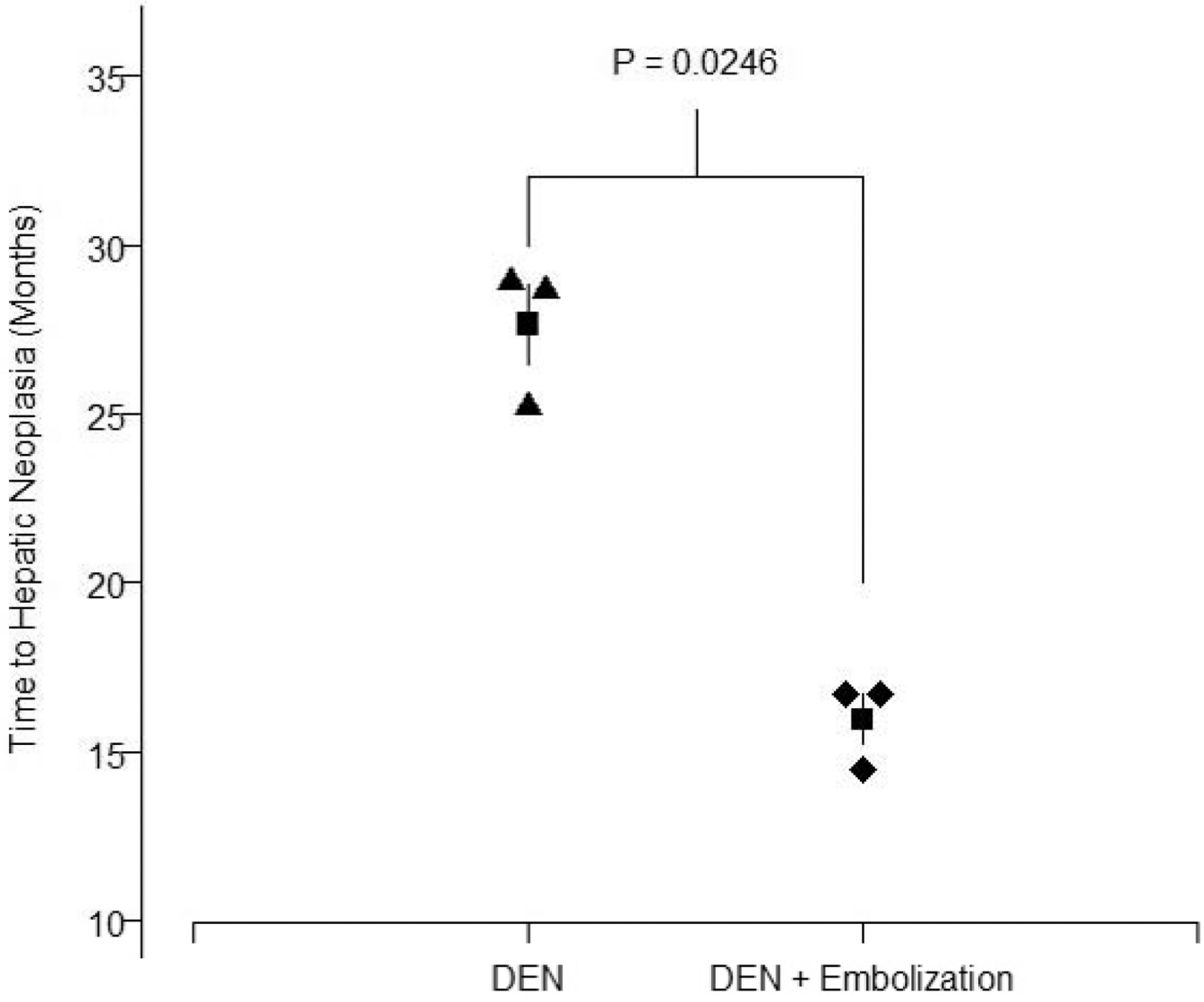


**Fig. 3. Time to hepatic neoplasia in diethylnitrosamine (DEN)-treated Yucatan miniature pigs**

In the group receiving DEN only (black triangles), the mean time to hepatic neoplasia (i.e., hepatic adenoma or hepatocellular carcinoma) was 27.65 ± 2.07 months (black square) with a range of 25.26–28.98 months. In the group receiving DEN + partial liver embolization (black diamonds), the mean time to hepatic neoplasia was 15.97 ± 1.28 months (black square) with a range of 14.49–16.72 months.

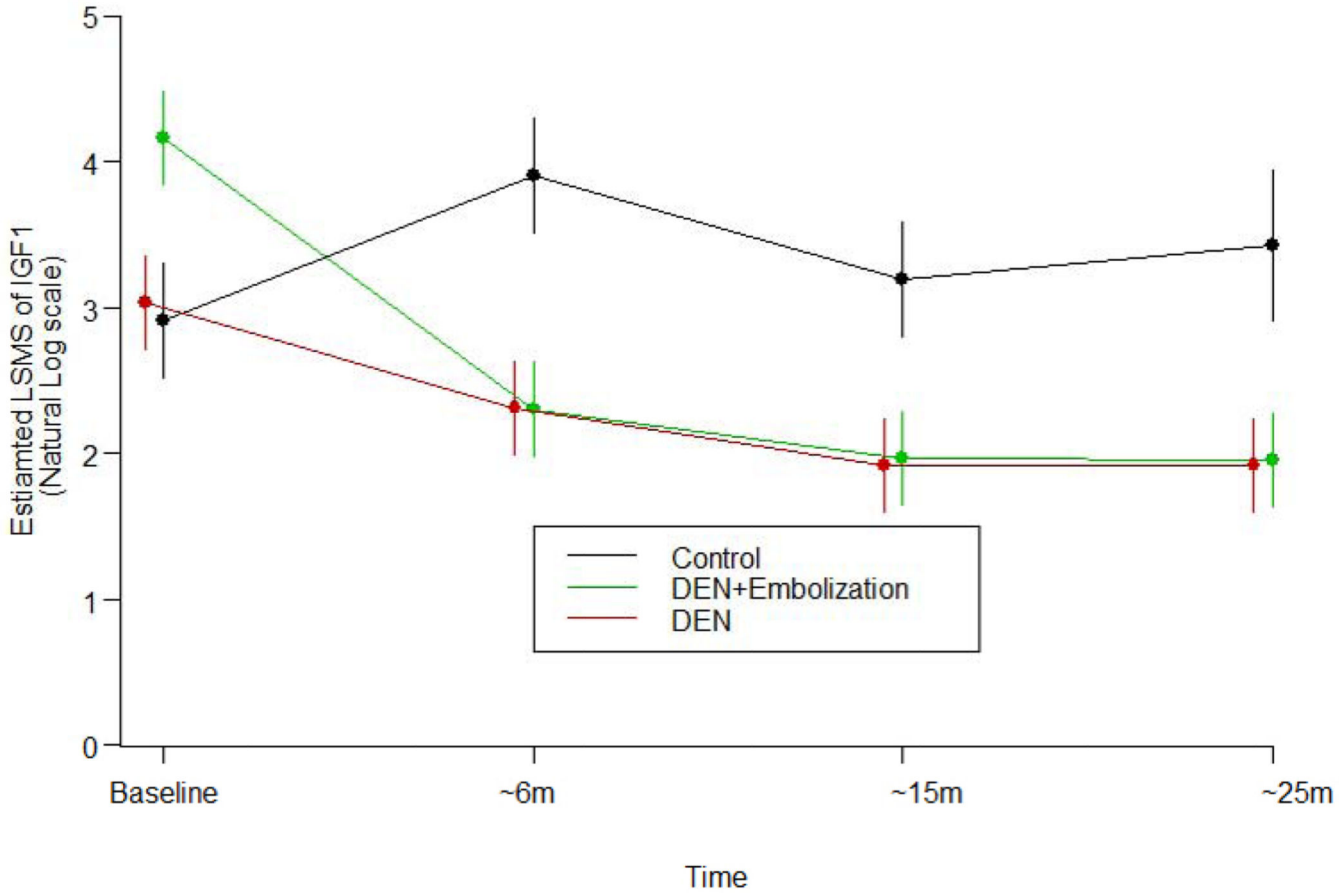


**Fig. 4. Estimated least square means (LSMS) of IGF1 from baseline to 25 months with standard error**

In both diethylnitrosamine (DEN)-treated groups, IGF1 expression significantly decreased over time when compared with the baseline value ($p<0.05$). However, no decreases were observed in the control pigs ($p<0.05$).

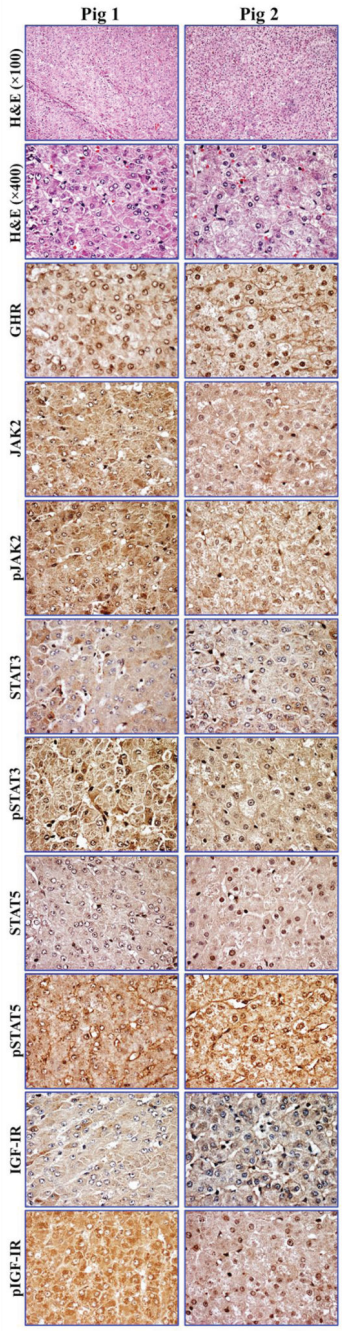


**Fig. 5. Expression of survival-promoting proteins in hepatocellular carcinoma (HCC) from two Yucatan miniature pigs**

Hematoxylin and eosin staining shows HCC arising in the livers from two different pigs (original magnifications, ×100 and ×400). Immunohistochemical staining shows the expression of GHR, JAK2, STAT3, STAT5, and IGF-IR in the HCC developed in our model. In addition, the expression of the phosphorylated/activated forms of these proteins including pJAK2, pSTAT3, pSTAT5, and pIGF-IR in HCC is also pronounced (original magnification, ×400).

**Table 1**

**Estimated Spearman correlation coefficients**

Estimated Spearman correlation coefficients between biomarkers in Yucatan miniature pigs.

| | GH | IGF1 | IGF2 | AFP | VEGF | IL-6 |
|---|---|---|---|---|---|---|
| **GH** | 1 | 0.039 (p=0.833) | 0.051 (p=0.786) | 0.425 (p=0.017) | −0.320 (p=0.080) | −0.151 (p=0.417) |
| **IGF1** | | 1 | 0.093 (p=0.620) | −0.310 (p=0.090) | −0.164 (p=0.377) | −0.172 (p=0.356) |
| **IGF2** | | | 1 | 0.023 (p=0.904) | 0.363 (p=0.045) | 0.137 (p=0.461) |
| **AFP** | | | | 1 | 0.090 (p=0.962) | −0.056 (p=0.767) |
| **VEGF** | | | | | 1 | 0.516 (p=0.003) |
| **IL-6** | | | | | | 1 |

GH and AFP had a positive correlation coefficient of 0.425 (p=0.017), and VEGF and IL-6 had a positive correlation with an estimated coefficient of 0.516 (p=0.003).